

Supporting Information for

Electrocatalytic hydrogen evolution from neutral water by molecular cobalt tripyridine-diamine complexes

Peili Zhang,^a Mei Wang,^{*a} Frederic Gloaguen,^{*b} Lin Chen,^a François Quentel^b and Licheng Sun^{*ac}

^a *State Key Laboratory of Fine Chemicals, DUT-KTH Joint Education and Research Centre on Molecular Devices, Dalian University of Technology (DUT), Dalian 116024, P.R. China. E-mail: symbueno@dlut.edu.cn*

^b *UMR 6521, CNRS, Université de Bretagne Occidentale, CS 93387, 29238 Brest, France. E-mail: fgloague@univ-brest.fr*

^c *Department of Chemistry, KTH Royal Institute of Technology, Stockholm 10044, Sweden*

Received (in XXX, XXX) Xth XXXXXXXXX 20XX, Accepted Xth XXXXXXXXX 20XX

DOI: 10.1039/b000000x

Materials and instruments

Materials. All manipulations were carried out at room temperature under a dinitrogen atmosphere or using high-vacuum Schlenk techniques unless otherwise noted. Diethyl ether and tetrahydrofuran were dried over activated 4 Å molecular sieves for 1 day and then distilled over sodium under nitrogen atmosphere. Acetonitrile and methylene dichloride were distilled over CaH₂ and stored under a dinitrogen atmosphere. Water was deionized with the Millipore Milli-Q UF Plus system. Electronic grad Hg (99.999%) was purchased from Aladdin, glass carbon rods, and platinum gauze were purchased from BASi for the electrochemical studies. Other commercially available chemicals such as Co(BF₄)₂·6H₂O, benzaldehyde, benzyl chloride, 1,2-ethanediamine, 1,3-propanediamine, and 2-(chloromethyl)pyridine hydrochloride were purchased from local suppliers and used as received.

Instruments. NMR Spectra were collected with a varian INOVA 400 NMR spectrometer. Mass

spectra were determined by Waters/Micromass LC/Q-TOF-MS. Elemental analyses were performed with a Thermoquest-Flash EA 1112 elemental analyzer.

Synthesis

Syntheses of bztpen and bztpnn ligands. tripyridine-diamine ligands *N*-benzyl-*N,N',N'*-tris(2-pyridylmethyl)ethylenediamine (bztpen) and *N*-benzyl-*N,N',N'*-tris(2-pyridylmethyl)propylenediamine (bztpnn) was prepared according to the literature procedures.^{S1,S2}

bztpen: Anal. Calcd for C₂₇H₂₉N₅ (%): C 76.56, H 6.90, N 16.53; found: C 76.70, H 6.84, N 16.62. ¹H NMR (CDCl₃, 400 MHz): δ 8.48 (3H, m), 7.58 (3H, t), 7.47 (3H, t), 7.18–7.30 (5H, m), 7.12 (3H, m), 3.77 (4H, s), 3.72 (2H, s), 3.59 (2H, s) and 2.73 (4H, m). ¹³C NMR (CDCl₃, 400 MHz): δ 160.16, 159.73, 148.94, 148.79, 139.18, 136.30, 128.71, 128.17, 126.88, 122.71, 122.65, 121.84, 121.78, 60.78, 60.59, 58.91, 52.20 and 51.89. ESI-MS: Calcd for [M+H]⁺, *m/z* 424.24; found: 424.21.

bztpnn: Anal. Calcd for C₂₇H₂₉N₅ (%): C 76.85, H 7.14, N 16.00; found: C 76.83, H 7.12, N 16.03. ¹H NMR (CDCl₃, 400 MHz): δ 8.48 (3H, m), 7.60 (3H, t), 7.41 (3H, t), 7.18–7.30 (5H, m), 7.10 (3H, m), 3.75 (4H, s), 3.68 (2H, s), 3.56 (2H, s), 2.55 (2H, t), 2.48 (2H, t), 1.78 (2H, t). ¹³C NMR (CDCl₃, 400 MHz): δ 160.36, 159.91, 148.91, 148.73, 139.38, 136.33, 128.78, 128.17, 126.84, 122.78, 122.70, 121.83, 121.76, 60.42, 60.15, 58.60, 52.40, 51.91, 24.59. TOF-MS: Calcd for [M+H]⁺, *m/z* 438.2658; found: 438.1074.

Syntheses of [(bztpen)Co(NCCH₃)](BF₄)₂ (1). Compound Co(BF₄)₂·6H₂O (0.34 g, 1.0 mmol) was added to a acetonitrile solution (40 mL) of bztpen (0.43 g, 1.0 mmol). The mixture was stirred under nitrogen atmosphere at room temperature for 8 h. The brown solution was then concentrated to ~10 mL under vacuum and kept under nitrogen atmosphere at room temperature for 2 days. Rod-shape light brown crystals were obtained in a yield of 71% (0.5 g). Anal. Calcd for C₂₉H₃₂N₆B₂F₈Co (%): C 49.96,

H 4.63, N 12.05; found: C 49.96, H 4.60, N, 12.10. ^1H NMR (400 MHz, CD_3COCD_3): δ 1.88, 7.41, 11.40, 13.54, 35.12, 42.47, 61.58, 63.02. TOF-MS: Calcd for $[\text{M}-\text{CH}_3\text{CN}-\text{BF}_4]^+$ ($\text{C}_{27}\text{H}_{29}\text{BN}_5\text{F}_4\text{Co}$): m/z 569.1784; found: 569.1773.

Syntheses of $[(\text{bztpnn})\text{Co}(\text{NCCH}_3)](\text{BF}_4)_2$ (2**).** The preparation of **2** was made in the essentially identical way as that for **1** but using bztpnn as ligand. The product was obtained in a yield of 62% (0.43 g). Anal. Calcd for $\text{C}_{30}\text{H}_{34}\text{N}_6\text{B}_2\text{F}_8\text{Co}$ (%): C 50.67, H 4.82, N 11.82; found: C 50.58, H 4.77, N 11.85. ^1H NMR (400 MHz, CD_3COCD_3): δ 1.86, 7.30, 10.40, 14.05, 34.37, 47.97, 61.58. TOF-MS: Calcd for $[\text{M}-\text{BF}_4-\text{CH}_3\text{CN}]^+$ ($\text{C}_{28}\text{H}_{31}\text{N}_5\text{BF}_4\text{Co}$): m/z 583.1941; found: 583.1947.

Syntheses of $[(\text{bztpen})\text{Co}(\text{H}_2\text{O})](\text{BF}_4)_2$ (3**).** The preparation of **3** was made in the essentially identical way as that for **1** but using water as solvent. The product was obtained in a yield of 86% (0.58 g). Anal. Calcd for $\text{C}_{27}\text{H}_{31}\text{N}_5\text{OB}_2\text{F}_8\text{Co}\cdot\text{H}_2\text{O}$ (%): C 46.85, H 4.81, N 10.12; found: C 46.77, H 4.67, N 10.03. ^1H NMR (400 MHz, CD_3COCD_3): δ 3.88, 7.60, 12.10, 33.19, 44.42, 59.51, 62.13. TOF-MS: Calcd for $[\text{M}-\text{BF}_4-\text{H}_2\text{O}]^+$ ($\text{C}_{27}\text{H}_{29}\text{N}_5\text{BF}_4\text{Co}$): m/z 569.1784; found: 569.1777.

Syntheses of $[(\text{bztpnn})\text{Co}(\text{H}_2\text{O})](\text{BF}_4)_2$ (4**).** The preparation of **4** was made in the same way as that for **1** but using bztpnn as ligand and water as solvent. The product was obtained in a yield of 77% (0.53 g). Anal. Calc. for $\text{C}_{28}\text{H}_{33}\text{N}_5\text{OB}_2\text{F}_8\text{Co}\cdot\text{H}_2\text{O}$ (%): C 47.24, H 4.90, N 10.02; found: C 47.12, H 4.82, N 9.93%. ^1H NMR (400 MHz, CD_3COCD_3): δ 2.08, 7.16, 10.98, 33.19, 48.42, 55.11, 61.75. TOF-MS: Calcd for $[\text{M}-\text{BF}_4-\text{H}_2\text{O}]^+$ ($\text{C}_{28}\text{H}_{31}\text{N}_5\text{OBF}_4\text{Co}$): m/z 583.1941; found: 583.1942.

Crystallographic structure determinations

The single-crystal X-ray diffraction data were collected with an Bruker Smart Apex II CCD diffractometer with a graphite-monochromated $\text{Mo}-K_\alpha$ radiation ($\lambda = 0.071073 \text{ \AA}$) at 293 K using the ω - 2θ scan mode. Data processing was accomplished with the SAINT processing program.^{S3} Intensity

data were corrected for absorption by the SADABS program.^{S4} All structures were solved by direct methods and refined on F^2 against full-matrix least-squares methods by using the SHELXTL 97 program package.^{S5} All non-hydrogen atoms were refined anisotropically. Hydrogen atoms were located by geometrical calculation. Crystallographic data and selected bond lengths and angles for **1–4** are given in Tables S1, S2 and S3. Molecular structures of **1–4** are given in Figs. 2, S1 and S2. CCDC-937142 (**1**), -937144 (**2**), -937143 (**3**), and -937145 (**4**), contain the supplementary crystallographic data for this paper. These data can be obtained free of charge from The Cambridge Crystallographic Data Centre via www.ccdc.cam.ac.uk/data_request/cif.

Table S1 Crystallographic data and processing parameters for **1–4**

Complex	1	2	3	4
Formula	C ₂₉ H ₂₉ N ₆ CoB ₂ F ₈	C ₃₀ H ₃₁ B ₂ CoF ₈ N ₆	C ₂₇ H ₃₁ B ₂ CoF ₈ N ₅ O	C ₂₈ H ₃₀ N ₅ CoB ₂ F ₈ O
Formula weight	694.16	708.16	672.18	686.13
<i>T</i> / K	296	296	296	296
Crystal system	monoclinic	monoclinic	monoclinic	monoclinic
Space group	<i>P</i> 2(1)/ <i>n</i>	<i>P</i> 2(1)/ <i>n</i>	<i>P</i> 2(1)/ <i>n</i>	<i>P</i> 2(1)/ <i>n</i>
<i>Z</i>	4	4	4	4
<i>a</i> / Å	11.1909(3)	11.183(3)	11.4253(5)	11.2389(6)
<i>b</i> / Å	23.6444(7)	23.646(7)	23.1813(10)	23.3087(13)
<i>c</i> / Å	12.9931(4)	13.366(4)	13.1097(6)	13.5001(7)
<i>α</i> / deg	90	90	90	90
<i>β</i> / deg	112.386(2)	114.089(4)	111.606(3)	112.129(3)
<i>γ</i> / deg	90	90	90	90
<i>V</i> / Å ³	3178.91(16)	3226.8(16)	3228.2(3)	3276.0(3)
<i>D</i> _{calcd} / g m ^{−3}	1.457	1.458	1.486	1.395
<i>μ</i> / mm ^{−1}	0.617	0.610	0.619	0.599
<i>θ</i> Range / °	1.90–25.00	1.88–27.60	1.89–25.00	2.14–25.00
<i>F</i> (000)	1428	1448	1476	1412
GOF on <i>F</i> ²	1.079	1.060	1.103	1.075
Final <i>R</i> ₁ (<i>I</i> > 2σ(<i>I</i>))	0.0614	0.0711	0.0842	0.1089
Final <i>wR</i> ₂ (<i>I</i> > 2σ(<i>I</i>))	0.1827	0.2182	0.2538	0.1961

$$R_1 = \Sigma ||F_o| - |F_c|| / \Sigma |F_o|, \quad wR_2 = [\Sigma (|F_o|^2 - |F_c|^2)^2 / \Sigma (F_o^2)]^{1/2}$$

Table S2 Selected bond lengths (Å) and angles (deg) for **1** and **2**

Complex	1	2
Bond lengths		
Co–N1	2.125(3)	2.117(3)
Co–N2	2.104(3)	2.132(3)
Co–N3	2.186(3)	2.218(3)
Co–N4	2.181(3)	2.223(3)
Co–N5	2.235(3)	2.159(3)
Co–N6	2.086(3)	2.185(3)
Bond angles		
N1–Co–N2	101.38(11)	93.55(12)
N1–Co–N3	78.26(11)	80.85(12)
N1–Co–N4	98.26(10)	99.00(11)
N1–Co–N5	172.49(10)	173.47(12)
N1–Co–N6	91.55(11)	88.73(12)
N2–Co–N3	76.72(12)	78.42(12)
N2–Co–N4	147.60(11)	165.08(11)
N2–Co–N5	86.11(11)	91.35(12)
N2–Co–N6	103.11(13)	95.77(13)
N3–Co–N4	82.42(11)	95.57(11)
N3–Co–N5	75.29(10)	104.39(12)
N3–Co–N6	169.48(12)	167.66(12)
N4–Co–N5	104.33(11)	76.80(11)
N4–Co–N6	101.84(13)	92.56(12)
N5–Co–N6	86.11(12)	86.49(13)

Table S3 Selected bond lengths (Å) and angles (deg) for **3** and **4**

Complex	3	4
Bond lengths		
Co–O1	2.046(4)	2.122(3)
Co–N1	2.126(4)	2.125(3)
Co–N2	2.112(4)	2.151(3)
Co–N3	2.174(4)	2.196(3)
Co–N4	2.198(4)	2.222(3)
Co–N5	2.215(4)	2.142(3)
Bond angles		
O1–Co–N1	93.32(18)	91.97(14)
O1–Co–N2	101.31(19)	92.85(13)
O1–Co–N3	171.32(19)	168.32(14)
O1–Co–N4	103.1(2)	94.51(13)
O1–Co–N5	84.38(19)	83.52(15)
N1–Co–N2	100.15(15)	90.07(12)
N1–Co–N3	78.70(15)	80.80(12)
N1–Co–N4	97.85(15)	98.83(11)
N1–Co–N5	172.38(15)	173.51(12)
N2–Co–N3	77.03(18)	78.09(12)
N2–Co–N4	148.60(17)	168.23(12)
N2–Co–N5	87.43(16)	94.80(13)
N3–Co–N4	81.57(18)	95.66(12)
N3–Co–N5	103.97(16)	104.38(12)
N4–Co–N5	75.68(15)	76.95(11)

Electrochemistry studies

CV measurements in CH₃CN and THF. Cyclic voltammetry experiments were carried out in a three-electrode cell under Ar using Metrohm potentiostat. The working electrode was a glassy carbon disc (diameter 3 mm) polished with 3 and 1 μm diamond pastes and sonicated in ion-free water for 15 min prior to use. The reference electrode was a non-aqueous Ag⁺/Ag (0.01 M AgNO₃ in CH₃CN) electrode and the counter electrode was platinum wire. A solution of 0.1 M *n*Bu₄NPF₆ (Fluka, electrochemical grade) in CH₃CN or THF was used as supporting electrolyte, which was degassed by bubbling with dry argon for 15 min before measurement. The ferricinium/ferrocene (Fc⁺⁰) couple was used as an internal reference and all potentials given in this work are referred to the Fc⁺⁰ potential ($E(\text{Fc}^{+/0}) = 0.64 \text{ V vs. SHE}$).

CV and DPP measurements in water. The cyclic voltammograms and differential pulse polarograms, were recorded on a PGSTAT100N potentiostat with a controlled-growth mercury electrode (drop size $\sim 0.4 \text{ mm}^2$), a platinum wire auxiliary electrode, and an aqueous Ag/AgCl reference electrode. The solution was stirred constantly during controlled potential electrolysis experiments.

Controlled potential electrolysis experiments (CPE) in water. All CPE experiments made in water were carried out in a pear-shaped double-compartment cell except for measurements of Faradaic efficiency. A mercury pool with a surface area of 3.1 cm^2 was used as the working electrode for electrochemical studies conducted in aqueous media. Electrical contact of the mercury pool was achieved through a platinum wire immersed below the surface of the mercury. The auxiliary electrode, a 1 cm^2 platinum gauze, was placed in a column-shaped compartment with a bottom of porous glass frit (G3, 1.1 cm^2), which was inserted into the main chamber of the electrolysis experiment and fixed only $\sim 1 \text{ cm}$ above the surface of mercury pool electrode to reduce the internal resistance. The sample was bubbled with argon for 20 min before measurement and the electrolysis was carried out under argon

atmosphere. The solutions in both compartments were constantly stirred during electrolysis experiments. The reference electrode was a commercially available aqueous Ag/AgCl electrode and the potentials were reported with respect to SHE by adding 0.195 V to the experimentally measured values.

Bulk electrolysis. The controlled potential electrolysis experiments were conducted in a cell with the working electrode compartment containing 20–40 mL of 1.0 or 2.0 M phosphate buffer solution at pH 7 and the counter electrode compartment containing 5–10 mL of the same buffer used in the working electrode compartment. The volume of the gas generated during electrolysis experiment was quantified by a gas burette and the H₂ content was determined by GC analysis using a GC 7890T instrument with a thermal conductivity detector, a 5 Å molecular sieve column (2 mm × 5 m) and with N₂ as carrying gas. Each catalytic datum was obtained from at least two paralleled experiments.

Determination of Faradaic Efficiency. Gas chromatographic analysis of the electrolysis-cell headspace was made during the electrolysis of 2 µM solution of **3** in 30 mL of 1.0 M phosphate buffer at pH 7 in a gas-tight electrolysis cell at an applied potential of –1.25 V vs. SHE for 1 h with a mercury pool electrode (surface area 1 cm²). The amount of hydrogen generated was determined by the external standard method and the hydrogen dissolved in the solution was neglected. The generated H₂ volume is in good agreement with that calculated from consumed charge in the CPE experiment (Fig. S14)

References

- (S1) Lars Duelund, Rita Hazell, Christine J. McKenzie, Lars Preuss Nielsen and Hans Toftlund, *J. Chem. Soc., Dalton Trans.*, 2001, 152–156.
- (S2) (a) Mauro Vieira de Almeida, Ana Paula Soares Fontes, Richard Nilton Berg, Eloi Teixeira César, Emanuel de Castro Antunes Felício, and José Dias de Souza Filho. *Molecules* 2002, 7, 405-411). (b) Lars Duelund, Rita Hazell, Christine J. McKenzie, Lars Preuss Nielsen and Hans Toftlund, *J. Chem.*

Soc., Dalton Trans., 2001, 152–156.

(S3) G. M. Sheldrick, *SHELXTL97 Program for the Refinement of Crystal Structure*, University of Göttingen, Germany, 1997.

(S4) *Software packages SMART and SAINT*, Siemens Energy & Automation Inc., Madison, Wisconsin, 1996.

(S5) G. M. Sheldrick, *SADABS Absorption Correction Program*, University of Göttingen, Germany, 1996.

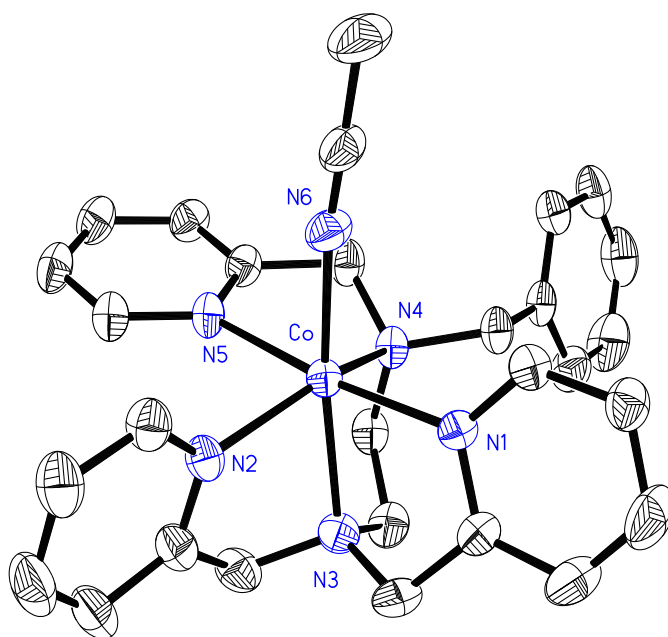


Fig. S1 Molecular structure of **1**. Anion, Solvent molecules and hydrogen atoms are omitted for clarity; thermal ellipsoids shown at 30% probability.

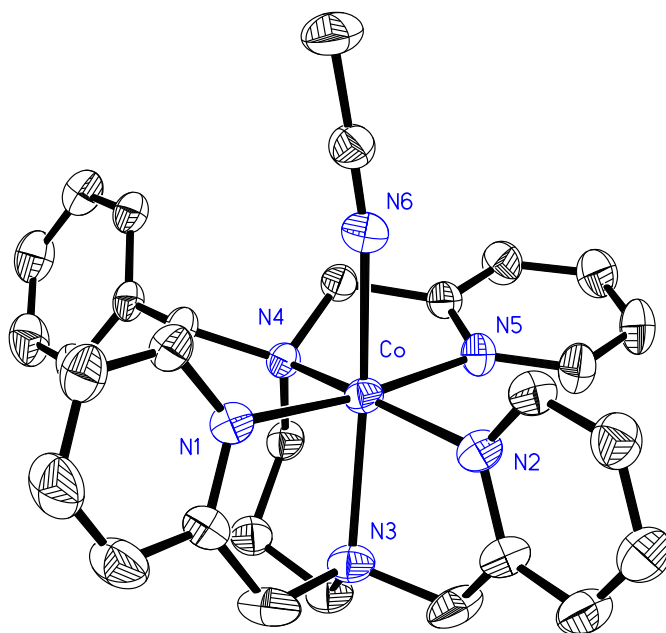


Fig. S2 Molecular structure of **2**. Anion, Solvent molecules and hydrogen atoms are omitted for clarity; thermal ellipsoids shown at 30% probability.

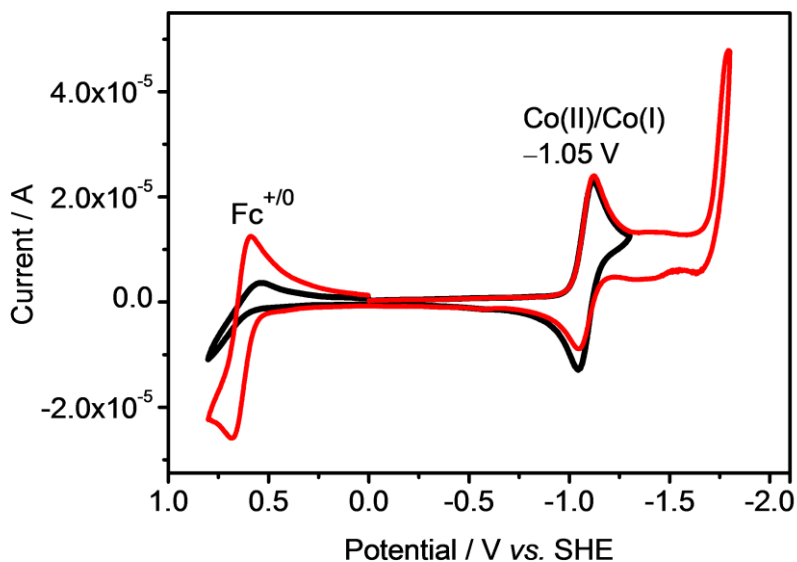


Fig. S3 Cyclic voltammograms of **1** in CH₃CN with (red) and without (black) the internal reference ($E(\text{Fc}^{+/0}) = 0.64 \text{ V vs. SHE}$; scan rate: 100 mV s^{-1}).

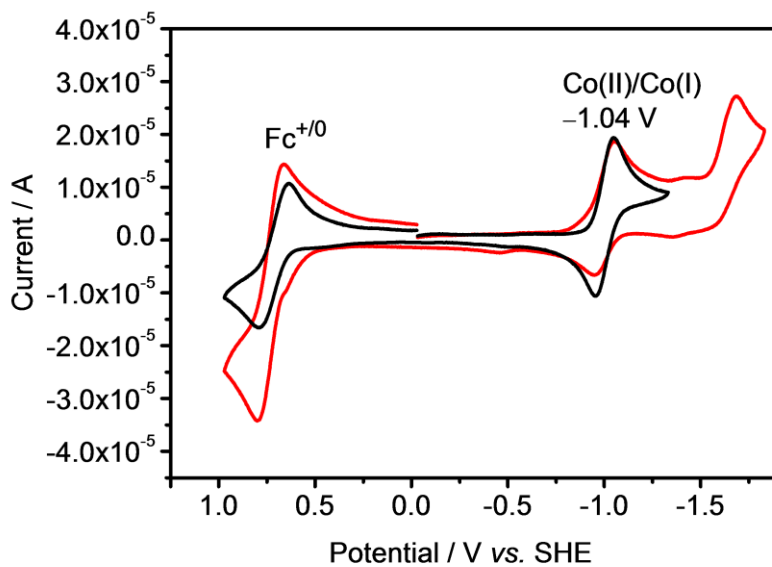


Fig. S4 Cyclic voltammograms of **1** in THF with (red) and without (black) the internal reference ($E(\text{Fc}^{+/0}) = 0.64 \text{ V vs. SHE}$; scan rate: 100 mV s^{-1}).

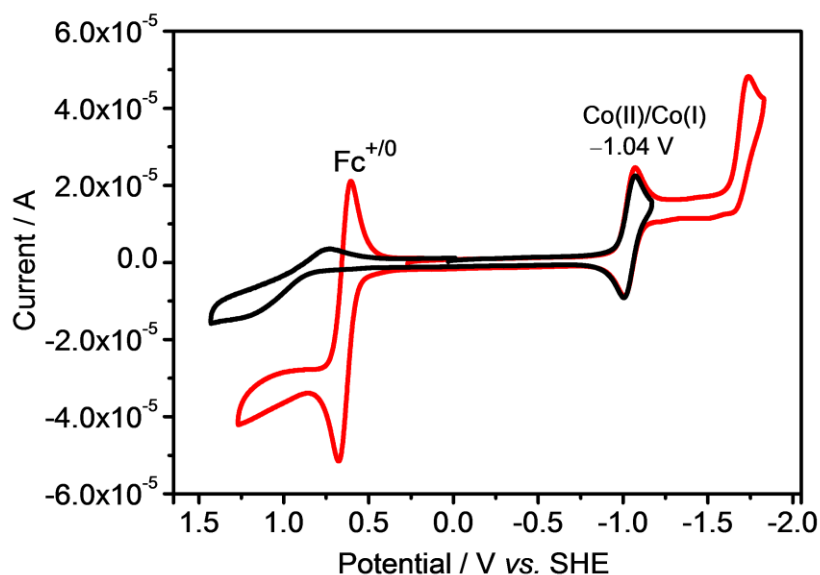


Fig. S5 Cyclic voltammograms of **2** in CH₃CN with (red) and without (black) the internal reference ($E(\text{Fc}^{+/0}) = 0.64 \text{ V vs. SHE}$; scan rate: 100 mV s^{-1})

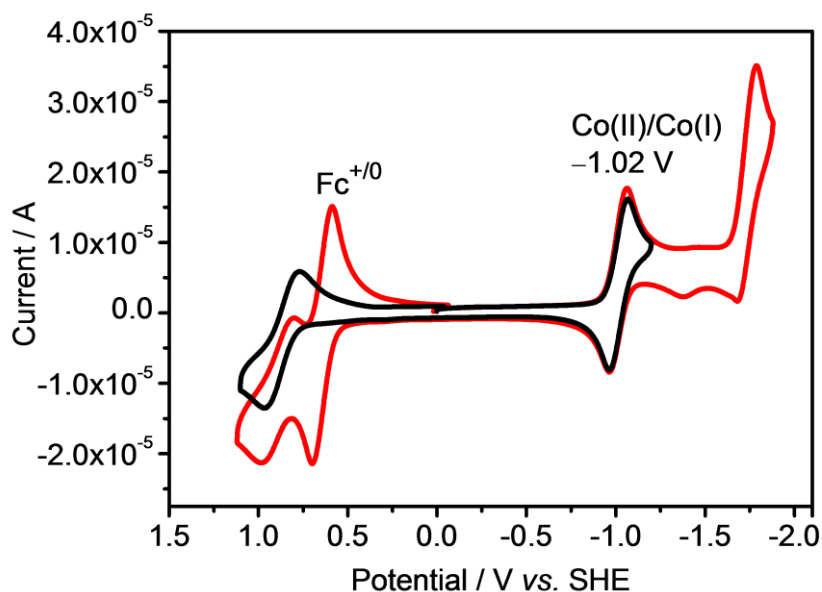


Fig. S6 Cyclic voltammograms of **2** in THF with (red) and without (black) the internal reference ($E(\text{Fc}^{+/0}) = 0.64 \text{ V vs. SHE}$; scan rate: 100 mV s^{-1}).

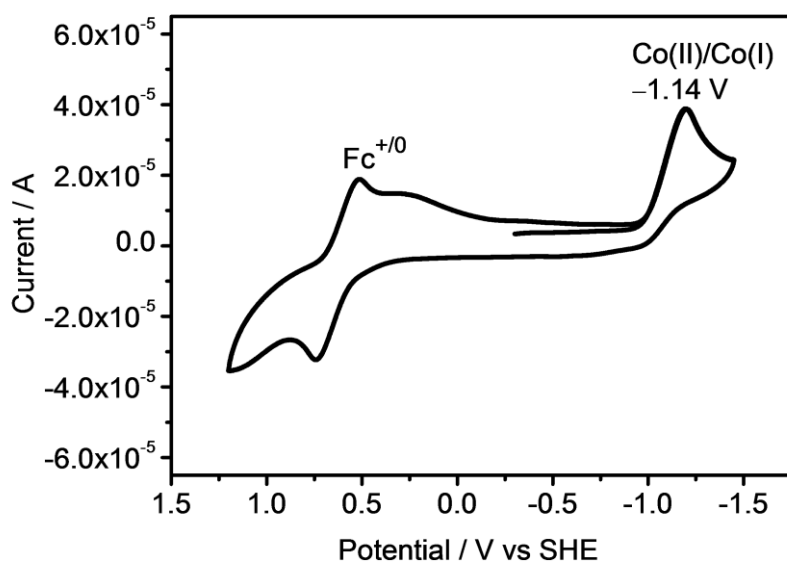


Fig. S7 Cyclic voltammogram of **3** in THF with internal reference ($E(\text{Fc}^{+/0}) = 0.64 \text{ V vs. SHE}$; scan rate: 100 mV s^{-1}).

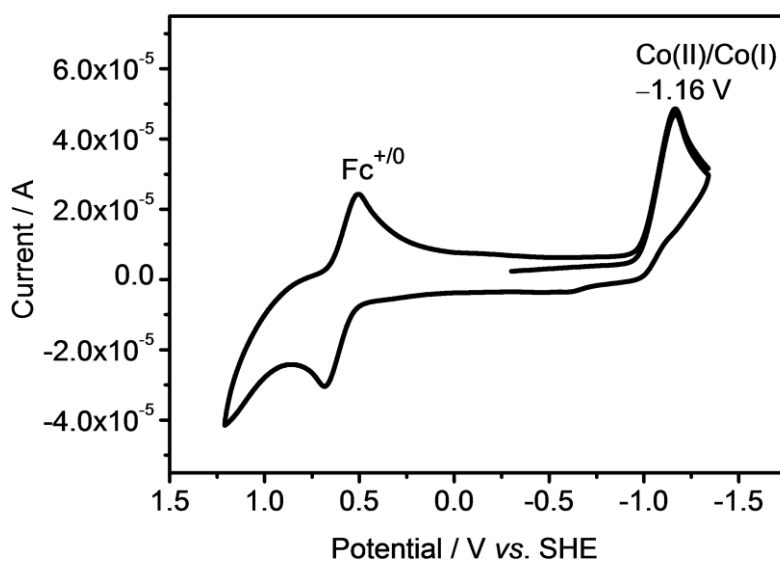


Fig. S8 Cyclic voltammogram of **4** in THF with internal reference ($E(\text{Fc}^{+/0}) = 0.64 \text{ V vs. SHE}$; scan rate: 100 mV s^{-1}).

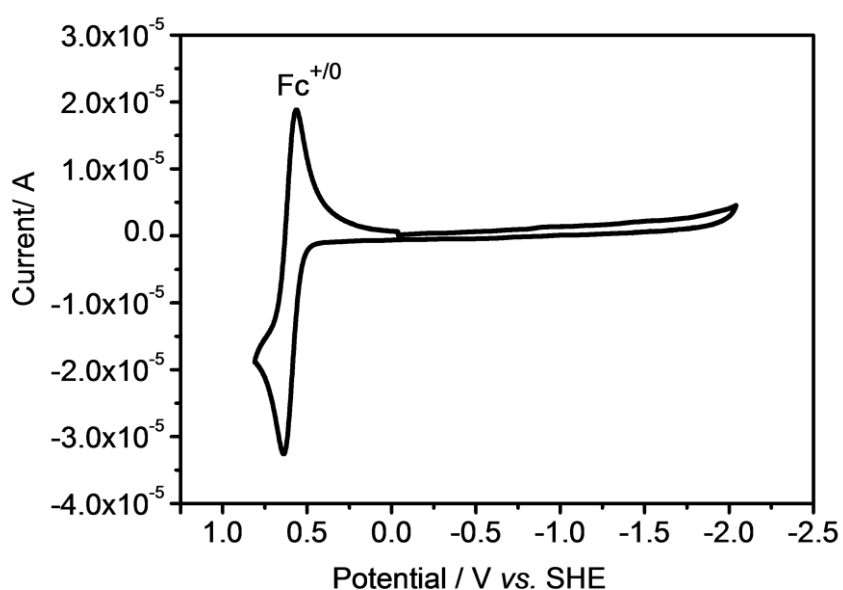


Fig. S9 Cyclic voltammogram of bztppen in CH_3CN and the ferrocene peak ($E(\text{Fc}^{+/0}) = 0.64 \text{ V vs. SHE}$) included as the reference (scan rate: 100 mV s^{-1}).

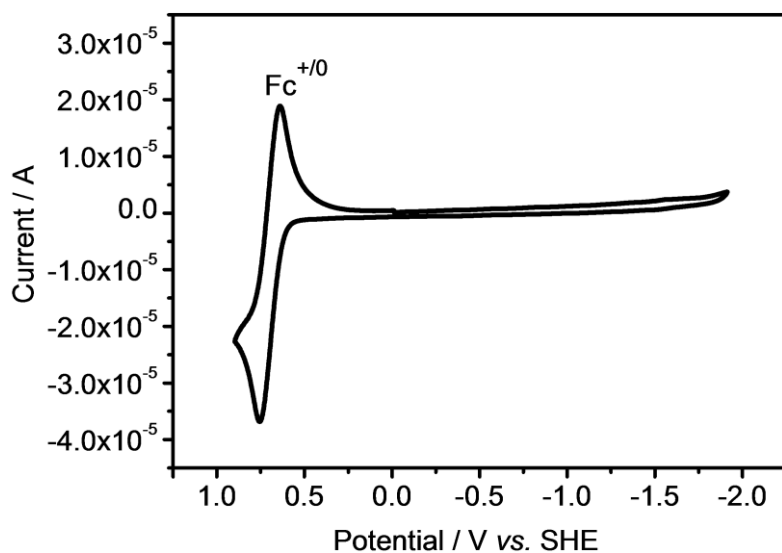


Fig. S10 Cyclic voltammogram of bztppn in CH_3CN and the ferrocene peak ($E(\text{Fc}^{+/0}) = 0.64 \text{ V vs. SHE}$) included as the reference (scan rate: 100 mV s^{-1}).

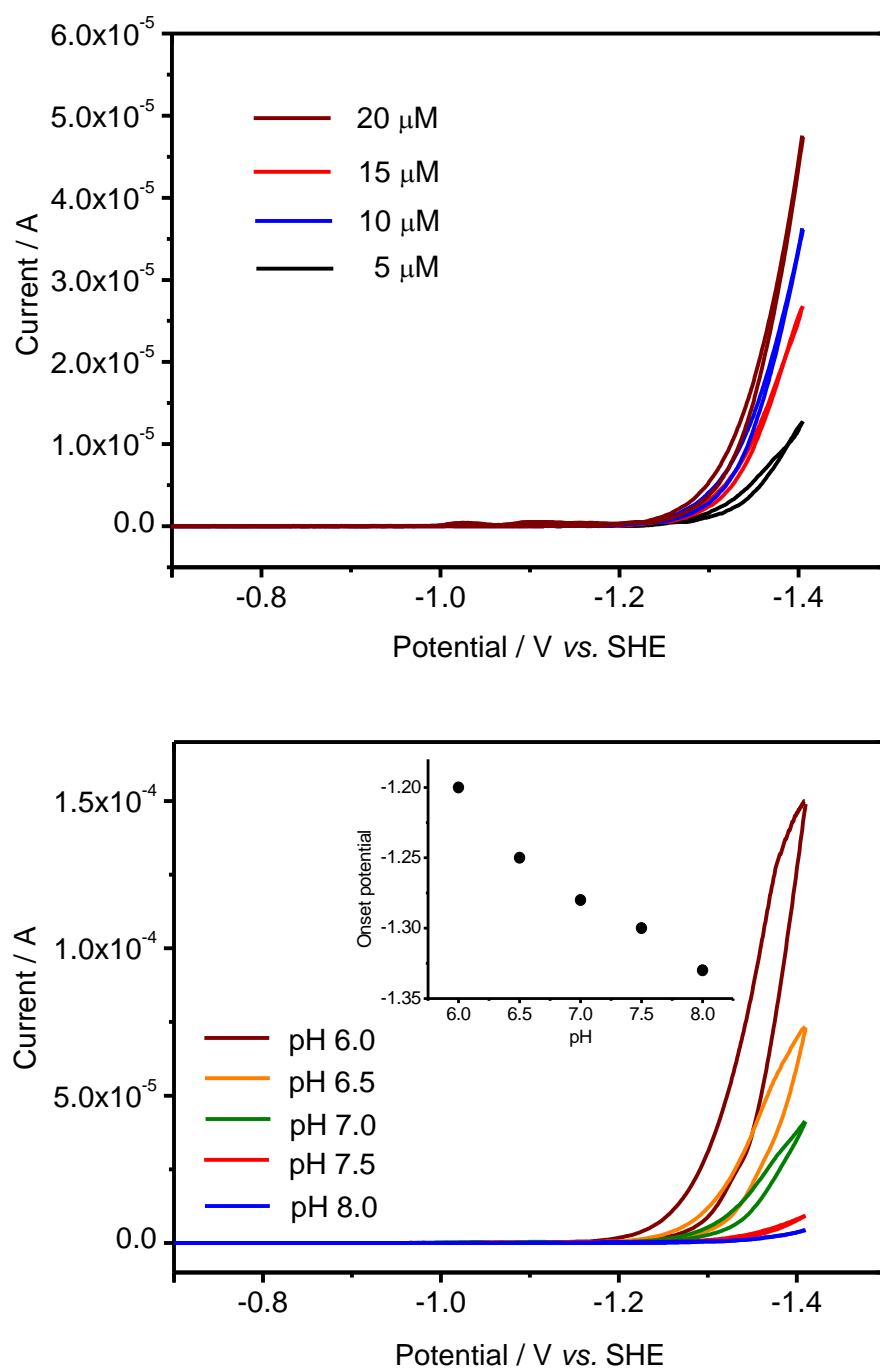


Fig. S11 (a) Cyclic voltammograms with varied concentrations of **bztpen** in 1.0 M phosphate buffer at pH 7; (b) Cyclic voltammograms of 15 μM **bztpen** with varied pH values in 1.0 M phosphate buffer, in a scan rate of 100 mV s^{-1} ; (Inset in Fig. S11b) Onset potential of the current of **bztpen** as a function of pH.

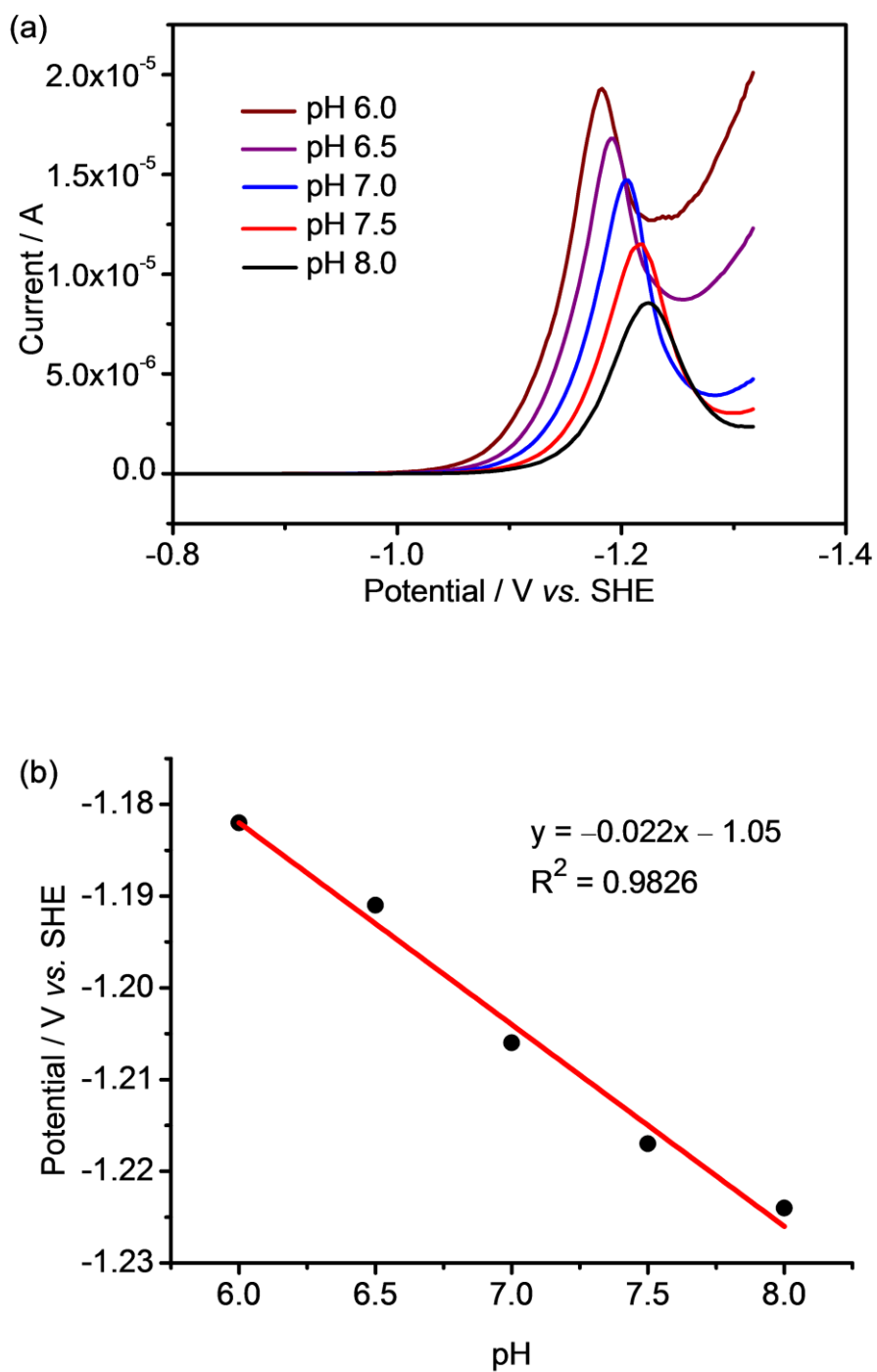


Fig. S12 (a) Differential pulse polarograms and (b) catalytic potential of **3** in 1.0 M phosphate buffer as a function of pH (scan rate: 100 mV s⁻¹).

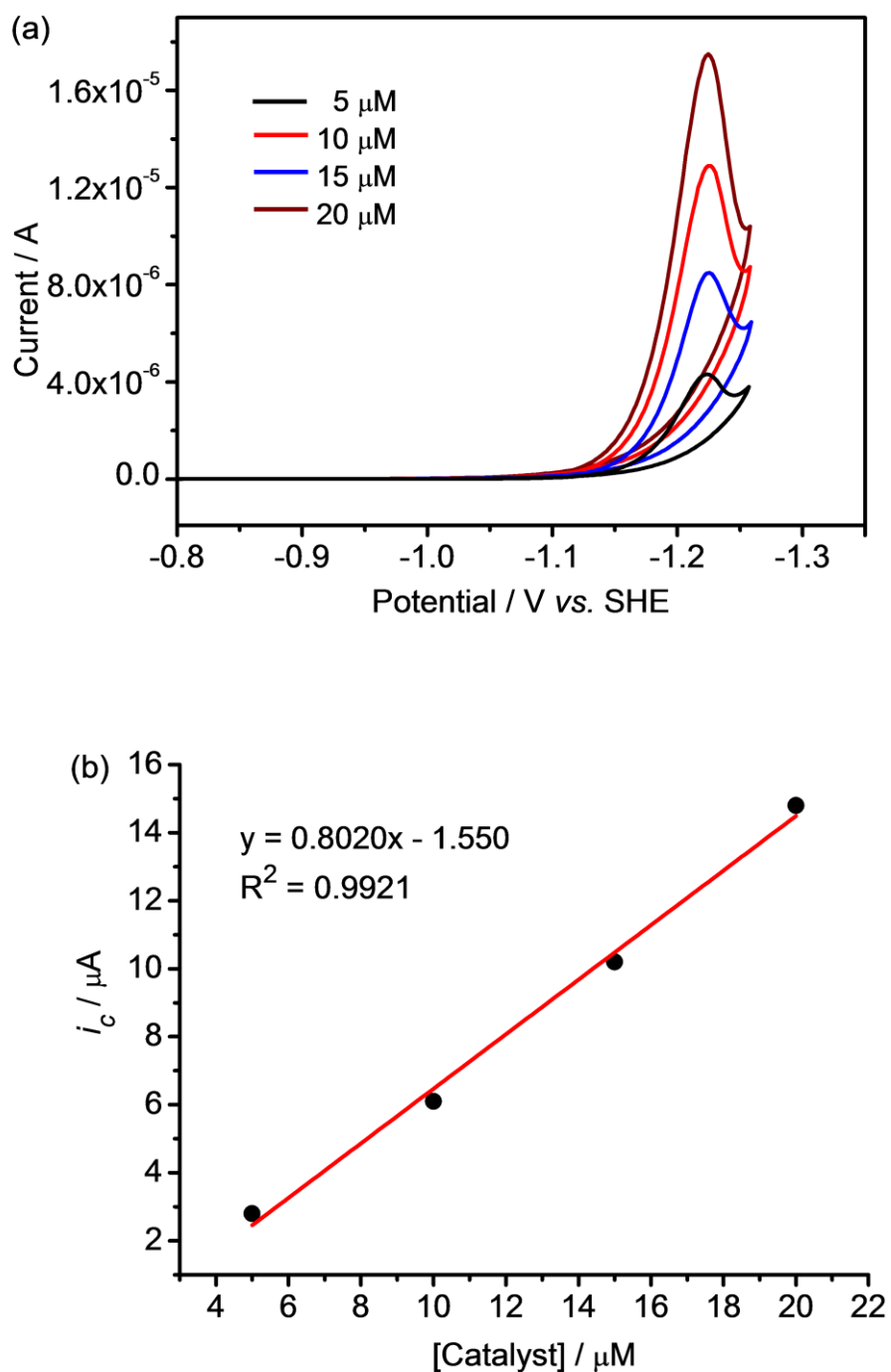


Fig. S13 (a) Cyclic voltammograms and (b) catalytic current maximum (i_c) of **3** in 1.0 M phosphate buffer at pH 7 as a function of the catalyst concentration (scan rate: 100 mV s^{-1}).

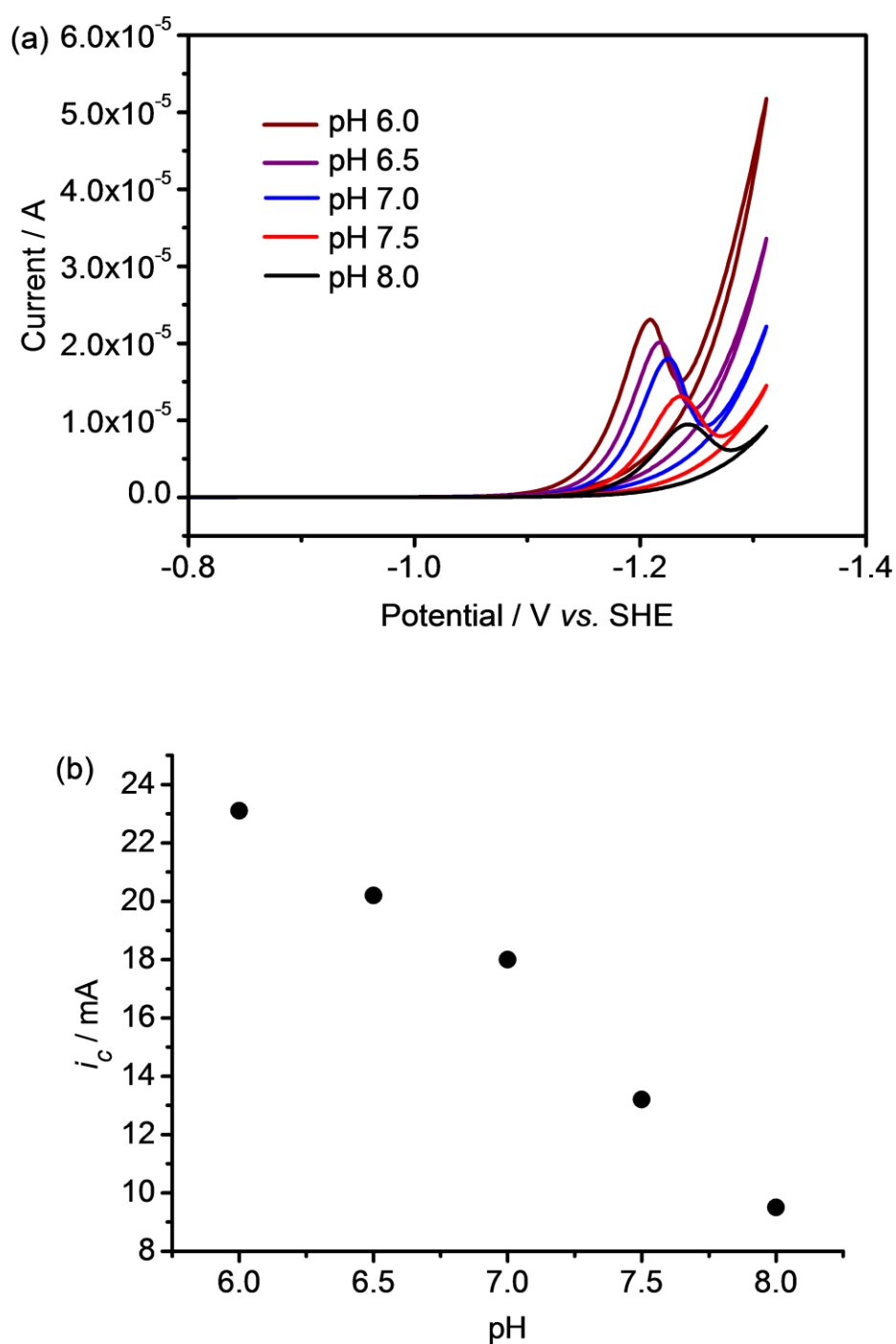


Fig. S14 (a) Cyclic voltammograms and (b) catalytic current maximum (i_c) of 15 μM **3** in 1.0 M phosphate buffer at pH 7 as a function of pH (scan rate: 100 mV s^{-1}).

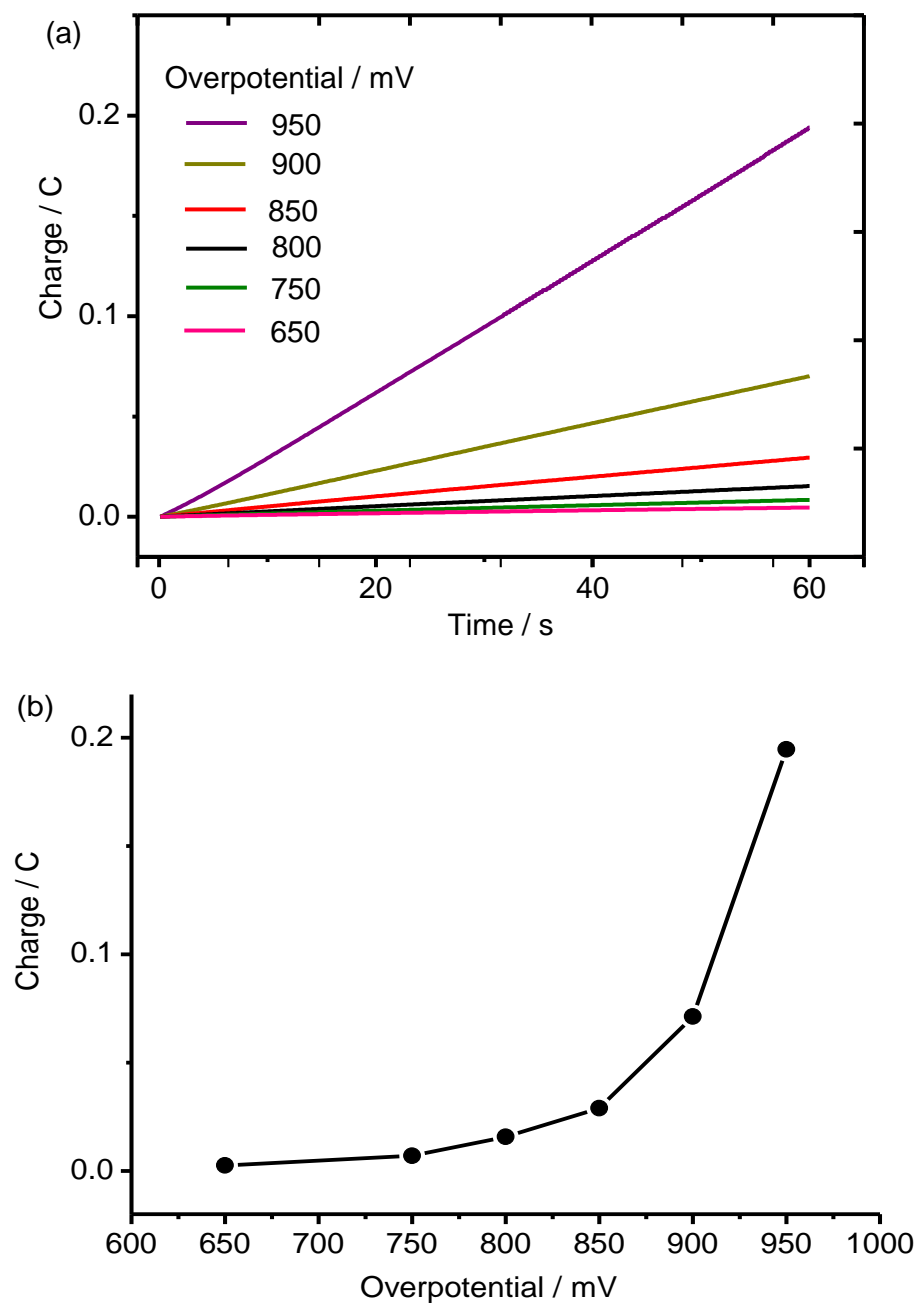


Fig. S15 (a) Charge build-up versus time and (b) the accumulated charge at the end of 1 min for the controlled potential electrolysis of a 5 μ M solution of **bztpen** in water buffered to neutral pH (1.0 M phosphate, pH 7) at various overpotentials.

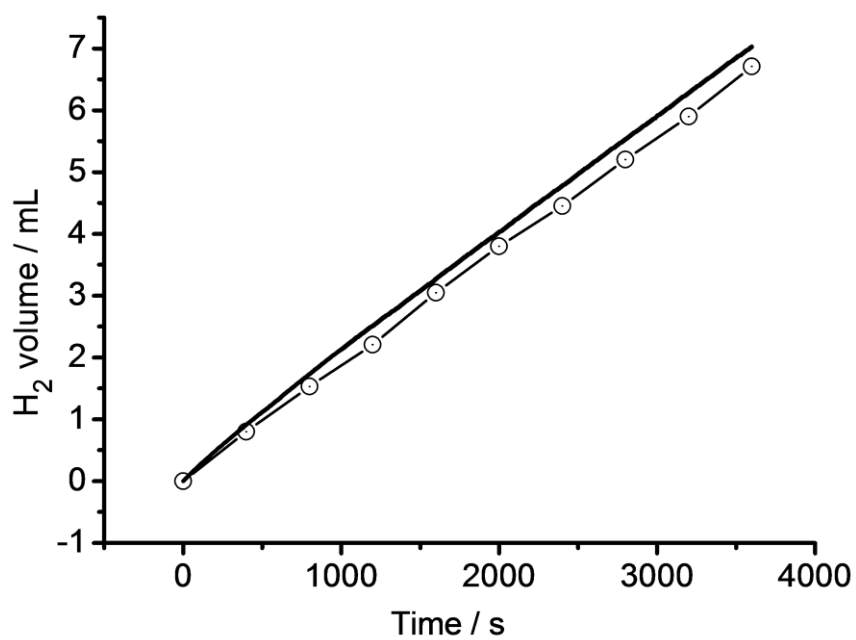


Fig. S16 The amount of hydrogen calculated from passed charge (black solid) and measured from gas chromatography (white circle) during the electrolysis of 2 μ M **3** in 1.0 M phosphate buffer at pH 7 with an applied potential of -1.25 V vs. SHE on a Hg pool electrode (1.0 cm^2).